

國立交通大學

土木工程學系

博士論文

空載光達率定與點雲匹配

On the Boresight Calibration and Point Cloud Matching of
Airborne LiDAR



研究生：劉榮寬

指導教授：史天元教授

中華民國九十四年七月



空載光達率定與點雲匹配

On the Boresight Calibration and Point Cloud Matching Airborne LiDAR

研 究 生：劉榮寬

Student: Jung-kuan Liu

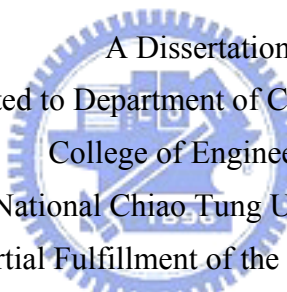
指導教授：史天元 博士

Advisor: Dr. Tian-yuan Shih

國立交通大學

土木工程學系

博士論文



A Dissertation
Submitted to Department of Civil Engineering
College of Engineering
National Chiao Tung University
in partial Fulfillment of the Requirements
for the Degree of
Doctor of Philosophy
in

Civil Engineering

July 2005

Hsinchu, Taiwan, Republic of China

中華民國九十四年七月



空載光達率定與點雲匹配

研究生: 劉榮寬

指導教授: 史天元 博士

國立交通大學
土木工程學系

摘要

空載光達系統（或稱為空載雷射掃描），為一種主動式之遙測技術用以快速獲取大量離散點三維坐標。空載光達系統的運作，基本上可視為透過快速旋轉反射鏡的雷射測距儀。由於其潛在之技術應用，使其在精度評估、資料校正（registration）及系統率定等相關議題上，吸引許多學者投入研究。空載光達點雲資料的系統誤差，其形成的原因很多，但主要來自於組成空載雷射掃描系統的三個子系統，亦即雷射測距系統（laser ranging system）、全球定位系統（GPS）以及導航系統（IMU）。本研究擬藉由系統率定、資料精度評估以及殘餘系統誤差消除等三個觀點，提出一套檢核空載光達資料精度的方法。

就系統率定而言，首先探討每一個軸角（boresight）率定參數，其參數特性對掃描精度之影像，以及率定的方法。本研究中，介紹二種目前商用空載光達系統的率定方法；另就其操作上之缺點，提出改進之建議，同時使用實際率定飛航資料進行評估此改進方法，是否可提高軸角率定參數精度。其次，為能驗證率定參數用於實際雷射掃描業務時之精度，避免內插原始雷射點雲資料，且冀望能同時評估重疊航帶間之平面與高程精度，本研究利用點雲匹配概念搜尋重疊航帶間之對應點，以評估資料精度。一種常用於三維面匹配（surface matching）之演算法—疊代最近點演算法（Iterative Closest Point, ICP）。使用兩組經地面參考資料檢驗精度等級不同之掃描資料測試，結果顯示，ICP 不僅能作為重疊航帶間之資料精度評估工具，同時也可以解決搜尋重疊航帶間對應點（correspondence problem）之問題，而這個問題在評估重疊空載雷射航帶間之精度及後續系統誤差改正時，為非常重要的一項課題。

當經由面匹配確認資料存在系統誤差時，最後一個步驟乃是利用航帶平差的概念，消除殘存之系統誤差。由於部分測試航帶內缺乏可供辨識之地面控制點資料，本研究分別採用三維相似轉換（亦即七參數轉換）及三參數航帶平差法，嘗試修正殘存之航帶系統誤差。同時，使用之輸入觀測資料，即是由前一步驟利用面匹配所獲得之對應點資料。

其次，利用三參數航帶平差法亦獲得與三維相似轉換近似之結果。因此，三參數航帶平差法除再次確認以面匹配所獲得之對應點資料可用作航帶平差中之共軛點外，也證實本法可吸收大部分之高程系統誤差。最後，歸結上述之研究成果，提出空載光達資料精度評估與系統誤差校正流程。



On the Boresight Calibration and Point Cloud Matching of Airborne LiDAR

Student: Jung-kuan Liu

Advisor: Dr. Tian-yuan Shih

Department of Civil Engineering
National Chiao Tung University

ABSTRACT

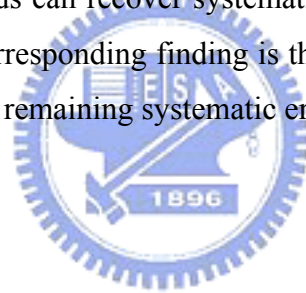
Airborne laser scanning (ALS), also known as “airborne LiDAR”, is an active remote sensing technique to capture surface terrain. The system is based on laser distance measurement, combined with a scanning mirror mechanism. As the potential of ALS becomes more promising, issues related to accuracy assessment, registration and data calibration receive increasing attention. Systematic errors in point clouds acquired by ALS may occur for many reasons. Three components of a laser system, namely, position (GPS), navigation (IMU), and range (laser scanner system), are sources of systematic errors. This dissertation presents a complete framework on handling the systematic errors in addressing system calibration, systematic error validation and remaining systematic error recovery.

For system calibration, each boresight misalignment parameter is discussed to assess its impact on data accuracy and methodology of recovery. The schemes on boresight calibration solution used by two different commercial systems are introduced and the improvement on one of these approaches is proposed. The in-situ data set from a calibration flight is used to evaluate the improvement on the accuracy of misalignment parameters. A surface matching method, i.e. the ICP algorithm, is proposed, for the validation of the calibrated point clouds. In addition, the ICP algorithm provides the benefit of avoiding the need to interpolate the raw laser points, and evaluating the height as well as the planimetry offsets from overlapping laser strips. To evaluate the performance of the algorithm across different data quality level, two data sets are tested. The results reveal that the ICP algorithm can be used to both quantify the

discrepancies from overlapping strips, and identify a solution regarding the correspondence problem.

The remaining systematic errors can be affirmed by using the proposed surface matching technique. Next, this research presents a strip adjustment procedure for the recovery of data with remaining systematic errors. Two methods are applied. The first one is the three-dimensional (3-D) similarity transformation, i.e. the seven-parameter transformation between two 3-D data sets. The second one is the strip adjustment using three parameters to adjust the laser strips when not enough ground reference points are available. Meanwhile, the corresponding points derived from ICP matching are used to form the observations to implement the adjustment.

The two proposed methods of strip adjustment confirm the following: (1) the corresponding points from ICP matching are sufficient to form the observations to implement adjustment; (2) the two methods can recover systematic error, especially on height. Analysis of the proposed solution on corresponding finding is then presented. Finally, a scheme on the accuracy assessment as well as remaining systematic errors recovery for ALS data is proposed.



**Dedicated to Jessica, my beloved wife.
Thank you for your love, support and
strength. This is your achievement as
well as mine.**





ACKNOWLEDGMENTS

First of all, I would like to give my sincere appreciation to my advisor, Professor Tian-Yuan Shih, who suggests the topic and leads me through this research by showing his unreserved kindness, guidance, patience and encouragement.

I wish to express my sincere appreciation to Professor Cheinway Hwang, who is continuously showing his heartfelt desire to share his light of knowledge and guiding me with simplicity and sincerity.

Thanks should also go to Professor Shue-Chia Wang, Professor Liang-Chien Chen, Professor Yi-Hsing Tseng, and Professor Shih-Lin Hung for serving in my candidacy as well as dissertation committee and carefully reading and providing comments concerning various aspects of this research.

I also wish to thank the faculty, staff, and students in the Department of Civil Engineering for creating and promoting a unique atmosphere of academic excellence and genuine friendliness.

Special thanks I owe to Prof. Rongxing Li and Dr. Kaichang Di, for sharing data with me, supporting the facilities, their helpful suggestions, and the invaluable discussions about aspects related to this research and other topics during my stay in the Mapping and GIS Laboratory of the Ohio State University, sponsored by National Science Council (Study Abroad Program).

I would like to acknowledge the support by the Ministry of Defense. I am particularly thankful to General Yang An-Kang, Col. Huang Cheng-Jer and Col. Hsu Jer-Ming for their efforts, which made my study possible.

I appreciate my colleagues in photogrammetry and mapping group: Jin-King Liu, Wei-Chen Hsu, Miao-Hsiang Peng and Chia-Sheng Shieh who have encouraged me, contributed to my understanding of the field and helped me with their insight.

I would also like to thank Dr. Gwendolyn Lee, a professor in University of Florida, for her help in improving the language of this manuscript, for her enlightening advice, and for her friendship.

On a more personal level, I wish to thank my parents and my parents in-law. Their love, care and support throughout the years and their sacrifice so as to put my studies on the very top of their priorities. Without them, my study would have been much more difficult to get to this stage.

Lastly, but clearly not the least, I would like to thank my wife, Jessica, for her love, for standing by me, for taking care of two lovely kids, Yvonne and Dillon, and for enduring my temper when my pressure went up. I wish that words could tell how grateful I am to her.

A very heartfelt THANK YOU to all of you for helping me to achieve this goal!

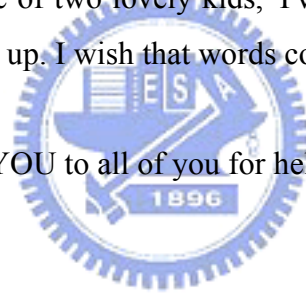
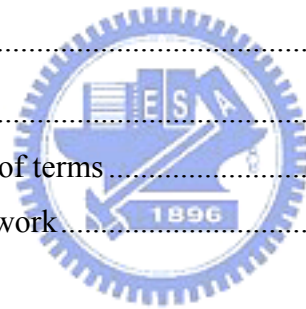


TABLE OF CONTENTS

	<u>Page</u>
Abstract (in Chinese).....	i
Abstract.....	iii
Dedication.....	v
Acknowledgments	vii
Table of contents	ix
List of Tables.....	xii
List of Figures.....	xiv
Chapter	
1 Introduction	1
1.1 Scope of this work	5
1.2 Glossary: Definition of terms.....	7
1.3 Organization of this work.....	8
2 Background.....	9
2.1 Airborne LiDAR.....	9
2.1.1 Ranging.....	10
2.1.2 Scanning	11
2.1.3 Position and orientation system.....	15
2.1.4 Determination of laser point.....	16
2.2 Potential error sources	16
2.2.1 Laser scanning system.....	16
2.2.2 Navigation system	18
2.2.3 Time error	21
2.2.4 Integration errors	22
2.3 Calibration problem.....	22



2.4	Systematic error validation.....	28
3	Motivation	30
3.1	Review of previous work.....	30
3.1.1	Calibration and strip adjustment.....	30
3.1.2	Accuracy assessment	39
3.2	The contribution of this research.....	42
4	Methodology.....	44
4.1	ALS boresight calibration.....	44
4.1.1	Mathematical model	44
4.1.2	Flight planning and observation collection	48
4.1.3	<i>Attune</i> program	51
4.1.4	Improvement on tie point selection	55
4.1.5	Boresight calibration steps for the Optech ALTM	60
4.2	Systematic error validation.....	63
4.3	Remaining systematic error recovery	68
4.4	ALS data pre-processing	70
4.5	Test data.....	70
4.5.1	ALS boresight calibration.....	71
4.5.2	Systematic error validation.....	72
4.5.3	Remaining systematic error recovery	76
5	Experiments and Results	77
5.1	Boresight calibration	77
5.1.1	Manual tie point selection.....	77
5.1.2	Tie point detection with image matching	82
5.1.3	Check by GCPs.....	92
5.1.4	Boresight calibration for the Optech ALTM	95
5.1.5	<i>TerraMatch</i>	98
5.2	Systematic error validation.....	99

5.2.1	Test site I (SI)	100
5.2.2	Test site II (SII)	105
5.3	Remaining systematic error recovery	108
5.3.1	3-D Similarity Transformation	108
5.3.2	Strip Adjustment with Three Parameters	113
6	Conclusion and Future Work	119
	Bibliography	123
	Appendix A Observation equation for boresight calibration	132
	Appendix B Height statistics for two test sites	137
	Appendix C Height differences between laser scanning data and GCPs	138
	Appendix D Correspondences from image matching vs. ICP registration	139
	Vita	144



LIST OF TABLES

Table	<u>Page</u>
2.1 Measured elevation offset versus torsion value.....	25
4.1 Flight parameters of boresight calibration.....	71
4.2 Technical parameters of the airborne laser scanning data for test sites.....	72
5.1 Initial tie point differences.....	78
5.2 Tie point differences after calibrated.....	79
5.3 Boresight parameters from manual tie point selection	79
5.4 The calibrated tie points difference from 3 operators.....	80
5.5 Tie point differences after calibrated with two kinds of grid size	81
5.6 Boresight parameters from manual tie point selection with two kinds of grid size ...	81
5.7 Initial tie point differences by using intensity images.....	89
5.8 Tie point differences after calibrated by using intensity images.....	89
5.9 Boresight parameters from image matching with intensity images	89
5.10 Initial tie point differences by using height images.....	91
5.11 Tie point differences after calibrated by using height images.....	91
5.12 Boresight parameters from image matching with height images	92
5.13 Height differences from laser points against GCPs by applying <i>Manual_cal</i>	93
5.14 Height differences from laser points against GCPs by applying <i>Auto_cal</i>	93
5.15 The correlation matrix for <i>Manual_cal</i>	94
5.16 The correlation matrix for <i>Auto_cal</i>	94
5.17 The correlation matrix based on tie point detection by using height images	94

5.18 Flight parameters of boresight calibration for the Optech ALTM	96
5.19 Boresight parameters from the Optech ALTM.....	96
5.20 Height differences from calibrated laser points against GCPs for Optech data.....	97
5.21 The initial misalignment angles for <i>TerraMatch</i>	98
5.22 Boresight misalignment angles from <i>TerraMatch</i>	98
5.23 Height differences from laser points against GCPs.....	99
5.24 The average height (μ , meters) and its standard deviation (σ , meters) in <i>SI</i>	101
5.25 Planimetry/height offset, applied to 8 patches of strip-8, 9, 10, and 11 for <i>SI</i>	102
5.26 Planimetry/height offset, applied to 13 patches of strip-1 and 2 for <i>SII</i>	106
5.27 The computed seven parameters for <i>SI</i>	110
5.28 Planimetric/height differences for strip 10 of <i>SI</i>	110
5.29 Height differences before and after data adjustment with GCPs for strip-10	111
5.30 The computed seven parameters for <i>SII</i>	111
5.31 Planimetric/height differences for strip 1 of <i>SII</i>	112
5.32 Height differences before and after data adjustment with GCPs for strip 1	113
5.33 The computed seven parameters for <i>SI and SII</i>	114
5.34 The mean height difference and RMSE for <i>SI and SII</i>	115

LIST OF FIGURES

Figure	<u>Page</u>
1.1 Effects of errors between two overlapping ALS strips.....	4
1.2 Overview of components of research	6
2.1 Basic components of an ALS system	9
2.2 Oscillating mirror scanning pattern (Carter et al., 2001).....	12
2.3 Nutating scanner pattern (Lohmann, 1999).....	13
2.4 Elliptical scanner pattern (Carter et al., 2001).....	14
2.5 Component Lag (Morin, 2002).....	17
2.6 Torsion error.....	18
2.7 Laser scanning system/IMU boresight (Mostafa, 2001)	19
2.8 Boresight induced errors.....	20
2.9 Boresight misalignment – roll	24
2.10 Torsion value versus elevation offset.....	25
2.11 Boresight misalignment – pitch.....	26
2.12 Boresight misalignment – heading	27
3.1 Strip coordinate frame	37
3.2 Ground control target for ALS (Csanyi, 2005)	39
3.3 Occlusion in the right strip at a building	41
4.1 Effects of roll error on overlapping data	49
4.2 Effects of pitch error on overlapping data.....	49
4.3 Effects of heading error on overlapping data	50

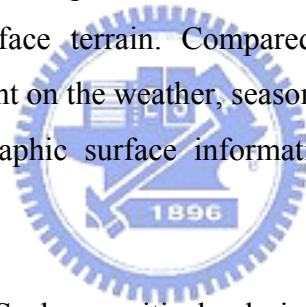
4.4 Optimal flight pattern for ALS calibration.....	51
4.5 Comparison of height and intensity data of ALS	53
4.6 A generated grayscale image from ALS intensity data	54
4.7 Road markings are selected as tie points	55
4.8 Work flow on the improvement of tie point selection for ALS calibration	60
4.9 Profile mode of scanning and calculating the correction for pitch.....	61
4.10 Calculating the correction for roll	62
4.11 Scale effect along the profile of runway.....	62
4.12 The ICP algorithm	67
4.13 A practical example for the ICP algorithm operation.....	67
4.14 The point clouds and intensity of the calibration strips.....	72
4.15 Two test sites for Systematic error validation	73
4.16 The average of height differences between laser points and GCPs for <i>SI</i> and <i>SII</i> ...	75
5.1 Manual selected tie point distribution	77
5.2 Profiles for uncalibrated and calibrated ALS strips.....	78
5.3 Intensity image with grid size smaller than average point density	82
5.4 The location and extent of each patch	82
5.5 The detected interest points for the 4th patch in two strips	83
5.6 The detected interest points for the 4th patch in two strips	84
5.7 Examples of incorrect matching	85
5.8 Examples of correct matching	86
5.9 The matched points in two overlapping strips from intensity image	87
5.10 Multiple point of 4th order in total interconnection (Kasser and Egels, 2002)	88
5.11 The matched points in two overlapping strips from height image	90
5.12 Profiles generated from calibrated ALS data	93

5.13 Boresight calibration data derived from the Optech ALTM 3070	95
5.14 Elevation differences coloring and building profile for Optech test data.....	97
5.15 Profiles of the building before and after calibrated of misalignment parameters	99
5.16 Four overlapping laser scanning strips in test site I (<i>SI</i>)	100
5.17 Along-track profile comparison from 3 overlapping strips for <i>SI</i>	102
5.18 Across-track profile comparison from 3 overlapping strips for <i>SI</i>	103
5.19 Trend of planimetry/height shifts for patch- 1 in <i>SI</i>	104
5.20 DSM of the integrating 4 overlapping strips of patch 1 in <i>SI</i>	105
5.21 Two overlapping laser scanning strips in test site II (<i>SII</i>)	105
5.22 Profile comparison from 2 overlapping strips for <i>SII</i>	107
5.23 DSM of the integrating 2 overlapping strips of patch 1 in <i>SII</i>	107
5.24 Corresponding points for patch 4 of <i>SI</i>	109
5.25 Two examples to show the model curve and data curve	109
5.26 A scaled symbol map using angle value (<i>SI</i>).....	111
5.27 A scaled symbol map using angle value (<i>SII</i>)	112
5.28 Height difference between original and transformed patch 2 (<i>SII</i>)	113
5.29 Residuals before and after strip adjustment for <i>SI</i>	115
5.30 Residuals before and after strip adjustment for <i>SII</i>	116
5.31 Work flows for accuracy assessment on ALS data	118

CHAPTER 1

INTRODUCTION

Airborne laser scanning (ALS), also known as “airborne LiDAR”, is an active remote sensing technique to capture surface terrain. The ALS system is based on laser distance measurement, combined with a scanning mirror mechanism. It measures the two-way travel time of the emitted laser pulses to determine the distance between the sensor and the ground (Wehr and Lohr, 1999). Integrated with a Global Positioning System (GPS) and an Inertial Measurement Unit (IMU), ALS can generate a three-dimensional, dense, geo-referenced point clouds for the reflective surface terrain. Compared to the traditional photogrammetric approach, ALS is less dependent on the weather, season, and time of the day in data collection, and can generate 3-D topographic surface information more rapidly (Ackermann, 1999; Baltsavias, 1999a).



The characteristics of ALS play a critical role in (i) mapping the fields with rapid and autonomous generation of digital surface model (Huising and Gomes Pereira, 1998), (ii) contributing towards autonomous surface reconstruction (Kraus and Pfeifer, 1997), and (iii) generating autonomous object recognition. One of the primary applications of ALS is to produce digital surface models (DSM). ALS observations have much more dense point spacing than the observations typically derived from photogrammetry (with current systems abilities exceeding 1 point/m²). When appropriate filtering algorithms are applied, ALS data can be classified as digital terrain models (DTM) and can be used for hydrological modeling (Brugelmann, 2000; Briese and Pfeifer, 2001). Other common uses of DTMs derived from ALS include applications in urban planning to project the impact of new building structures on light distribution in dense urban areas, or the impact of urban vistas (Haala and Brenner, 1999; Maas and Vosselman, 1999; Murakami et al., 1999; McIntosh et al., 2000).

In addition to the applications on DTMs, ALS has a unique ability to detect narrow linear features such as roads and rail lines (Berg and Ferguson, 2001). Of particular note is the ALS ability to measure power lines. Power lines, despite being small, have high reflectance with respect to laser energy. In addition to interacting with power lines, the transmitted energy can travel beyond power lines and reflect off the ground. This multiple return feature of ALS systems permits accurate modeling of power lines with respect to the ground, and measurement of the transmission towers (Terrasolid, 2004; Optech, 2004).

Next, an ALS system has a multiple return ability, which can be applied to biometric analysis. For several reasons, conventional mapping techniques in elevation measurement are insufficient to capture the textured pattern of the canopy and the occluded ground. First, when the laser energy is transmitted towards the forest, it will often hit the top of the tree canopy. Also, the laser signal has a small footprint to pass through the tree from the gaps of the leaves. In some cases the laser signal penetrates all the way to the forest ground. The observation set will describe the top and the shape of the tree canopies and the forest floor. The top and the ground information can be used to derive useful information for forest management (e.g., the count and determination of tree species, volume, and health), or fire management (e.g., behavior modeling) (Kraus and Pfeifer, 1998; Blair et al., 1999; Hofton et al., 2000; Sun and Ranson, 2000; Ziegler et al., 2001; Riano et al., 2003; Harding et al., 2004).

In order to reap the full benefits associated with various ALS applications, one key requirement is the high quality of input data. While the accuracy potential of ALS is high, to achieve high levels of accuracy, systematic errors in the input data need to be eliminated. For instance, the system vertical accuracy within a 15 cm range is consistently reported (Leica, 2004a), and the horizontal accuracy is the function of flight altitude (H), i.e. $H/2000$ m (Optech, 2002). However, prior research indicates that systematic errors remain in the data (Huising and Gomes Pereira, 1998; Crombaghs et al, 2000; Maas, 2002).

The contribution of this research is to develop a complete framework involving data processing techniques in addressing accuracy assessment as well as remaining systematic errors recovery for ALS data. While ALS systems have come a long way, the choice of

appropriate data processing techniques for particular applications is still being researched. Data processing, here, is understood as being either semiautomatic or automatic, and includes such tasks as “modeling of systematic error”, “filtering”, “feature detection”, and “thinning” (Axelsson, 1999; Lee, 2002; Sithole, 2003). Of these tasks, manual classification (filtering) and quality control pose the greatest challenge (Flood, 2001).

Systematic errors in point clouds acquired by ALS may occur for a wide variety of reasons (Huising and Gomes Pereira, 1998). They become most evident in adjacent overlapping strips. Systematic errors cause the ALS to report different height values, although the strips are in exactly the same planimetric location. Huising and Gomes Pereira (1998) also identified elevation errors in overlapping strips on the order of a few decimeters and planimetric errors of more than one meter. Systematic errors affect the laser data in several ways (Filin, 2003). They degrade the accuracy of the geo-location of the laser footprint, and they distort the surface that is reconstructed by the laser data.

Three components of a laser system, namely, position (GPS), navigation (IMU) and range (laser scanner system), are sources of systematic errors (Filin, 2001; Schenk, 2001; Maas 2002). Firstly, the mounting bias between the laser scanner reference system and the aircraft body frame is a major error source (Wehr & Lohr, 1999; Burman, 2000a; Filin, 2001; Morin & El-sheimy, 2002; Morin, 2002). A mounting bias causes the observed pointing direction of the laser beam to be different from the actual one. Secondly, a bias results in a measured range that is either systematically shorter or longer than the true value. The precision of slant distance measurement is primarily determined by the precision of time-of-flight measurement. With most systems operating at narrow opening angles, range biases propagate mainly into height coordinates. Next, the error budget of the scanning mirror is described by the angular resolution and may also be influenced by mechanical problems such as vibrations or oscillations. These errors will mainly propagate into the across-track planimetric coordinates (Maas, 2002). Other potential error sources are expected to have smaller effects. They include an error in determining the offset between the GPS and the laser system, time synchronization error between the laser scanner, IMU/GPS systems, IMU initialization error, and position offset (Filin, 2001).

Eliminating the systematic errors of ALS data requires suitable calibration procedures that combine laboratory calibration and in-flight calibration, or employs the strip adjustment to recover the remaining systematic errors. Performing in-flight system calibration is imperative because not only the location of the laser footprint can be more accurately identified, but also the systematic errors that distort the reconstructed surface form can be removed (Filin, 2001). A common problem of ALS data is that it shows systematic discrepancies in elevation and planimetric position when compared to other data source, such as ground check points. Systematic errors are largely due to an incorrect or incomplete calibration, though random errors exist in all sensor measurement. The effect of the errors can be easily revealed between two overlapping ALS strips (see Figure 1.1). Figure 1.1 depicts height discrepancies detected either by using shading relief presentation (Figure 1.1a), or by inspecting the profile from overlapping strips (Figure 1.1b).

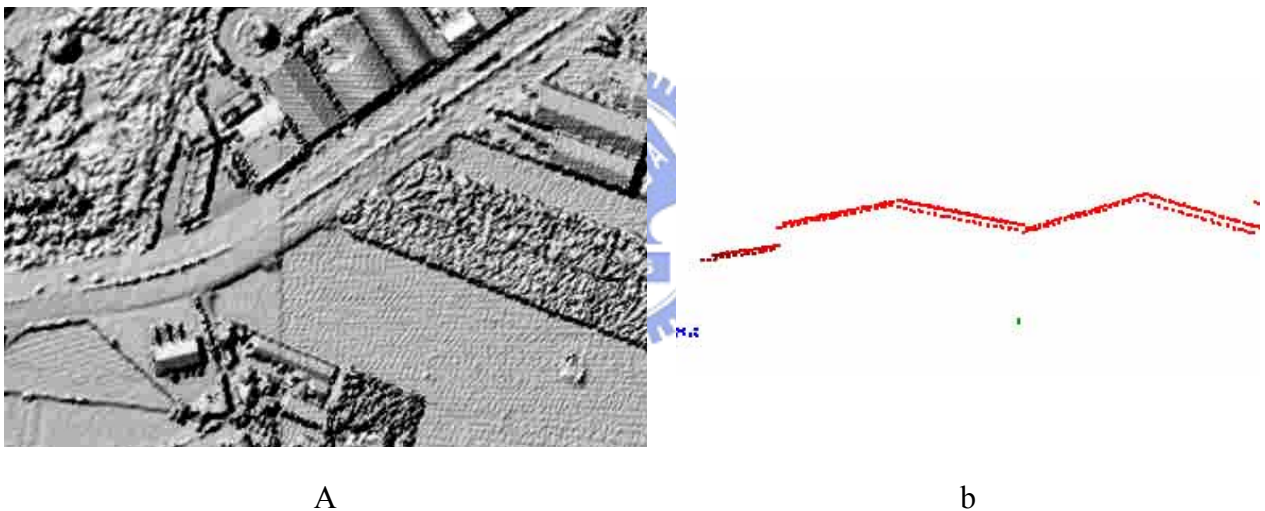


Figure 1. 1: Effects of errors between two overlapping ALS strips

The most common calibration method used in commercial ALS systems is a simple manual adjustment of the misalignment angles (Morin, 2002; Morin and El-Sheimy, 2002; Optech, 2003). Generally, the ALS system is calibrated by calibration flights (Burman, 2002; Kornus & Ruiz, 2003; Katzenbeisser, 2003) over a large building of known coordinates and over a flat surface (for example, an airport runway). The calibration results obtained over the past years show more or less stable values for the roll and pitch correction, while the scale factor and also the height offsets show a considerable variation over time (Kornus & Ruiz,

2003; Optech, 2003). Although practical, this method is time consuming, biased prone and requires ground control.

With laser data, no unique correspondence can be established between laser points and control points. Furthermore, the points derived from ALS systems are not necessarily on the physical surface but rather determined as a function of the distribution of backscattered energy (Filin et al., 2001). Thus, a control-point based calibration faces lots of difficulties. The calibration is a strategy. It is more than a formulation of the calibration equation. The identification of reference objects is very different from what is common practice in photogrammetry. Correspondence is a difficult problem to solve, particularly when the search space is big and the attribute that define the correspondence is difficult to assess. Therefore, it was usually left untreated or was simplified in manners that cannot be applied in general (Filin, 2001).

1.1 Scope of this work

The primary scope of this research is to present a complete framework on ALS system calibration, systematic error validation, and remaining systematic error recovery. The motivation lies in proposing a mechanism of quality control applied to ALS data for general use. Three phases of work are included in this research (see Figure 1.2).

The first phase reviews the current boresight calibration procedures on one of the main commercial ALS systems and proposes a strategy for improving the calibration. Morin (2002) developed and implemented a new calibration method for ALS systems. This new method will address the shortcomings in current manual methods by (i) discarding a need for ground control points, (ii) providing a rigorous stochastic model, (iii) modeling additional sources of error and, (iv) improving the speed of calibration. The ALS intensity is originally used to measure the correspondence between overlapping strips in Morin's (2002) work. This research enhances Morin's method on finding corresponding points (i.e. tie points) by proposing a surface-matching technique for an automatic tie point detection.

The second phase deals with the problems and methodologies to verify the calibrated ALS data on vertical discrepancies as well as horizontal shifts. Most of the work on accuracy

assessment for ALS data focuses on the height accuracy with ground check points. With the planimetric accuracy, it is usually much worse than height accuracy for an ALS system. The planimetric shifts of data have to be evaluated for the applications in need of higher planimetric accuracy, such as city modeling as well as biometric modeling. Therefore, a surface-matching algorithm is proposed in this phase to evaluate the quality of calibrated data. The scope of this phase covers not only a method to validate ALS data but also a solution to address the correspondence problem. The correspondence problem in overlapping ALS strips is a critical issue for accuracy assessment as well as systematic errors recovery.

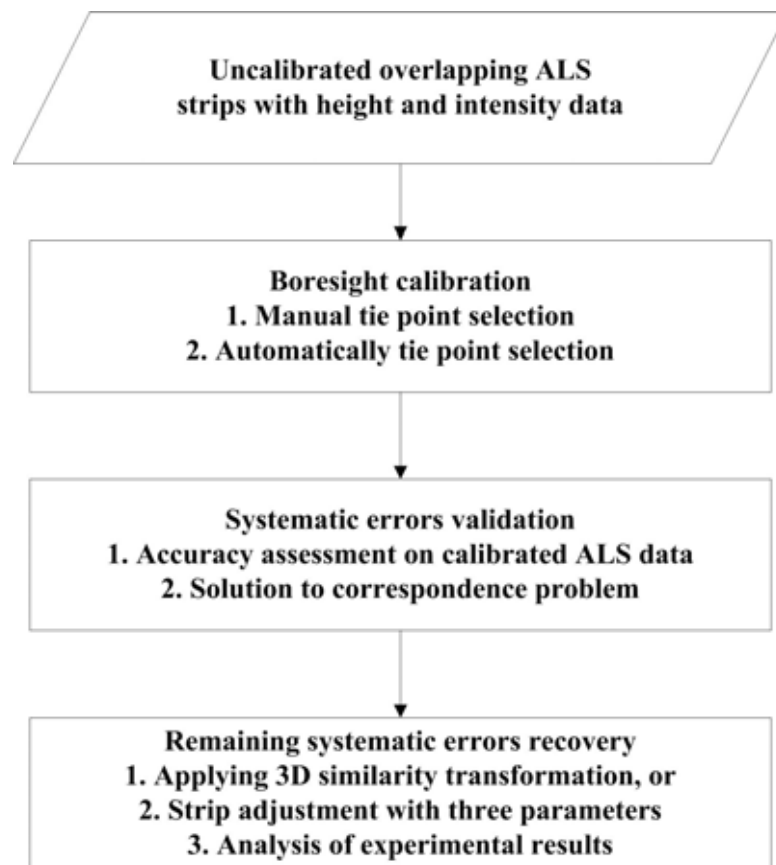


Figure 1. 2: Overview of components of research

In the last phase, two methods are presented to recover ALS strips that contain systematic errors. The 3-D similarity transformation -- the seven-parameter transformation between two 3-D data sets -- and the strip adjustment with three parameters are both used to recover the ALS strips when not enough ground reference data are available. The corresponding points

derived from the previous phase are used to form the observations in implementing the adjustment. Analysis of the proposed solution on corresponding finding is then carried out.

Figure 1.2 schematically depicts the main components of this research.

1.2 Glossary: Definition of terms

This section gives the definitions for some terms recurrently used throughout this dissertation.

- ALS - Airborne laser scanning (ALS), also known as airborne LiDAR (Light Detection and Ranging).
- Footprint – the area on the ground that is illuminated by the laser beam.
- Laser point – the ground positions (x, y, z-coordinates) computed by the ALS system. Position is a function of the measured range, attitude, position, and the system biases of the ALS at the time of ranging.
- DSM - Digital surface model is an elevation model of the earth's surface that can be manipulated by computer programs.
- DTM – Digital terrain model is an elevation model of the bare earth (with man-made structures, vegetation, etc. removed) that can be manipulated by computer programs.
- Strip - all point clouds taken within one ALS flight line.
- Tie point – 3-D coordinates often corresponding to the position of a physical detail of the scene, and seen in at least two images, or strips.
- Interest points – a point of the image around which the signal has specific characteristics, such as high values of the derivatives in several directions or at least two orthogonal directions, and detected by an interest point operator. These points are potentially useful for image matching.

- Height image - generates an image by using the height value of ALS point clouds as gray value.
- Intensity image – generates an image using the reflectance intensity of ALS point clouds to represent gray value.

1.3 Organization of this work

This dissertation is organized as follows. Chapter 2 provides information about ALS systems. System concepts and the description of fundamental components of an ALS are presented, followed by the effects of error regarding each component. The calibration problem related to ALS that focuses on the misalignment between the navigation and laser component is also presented.

Outlining the contribution of this dissertation, Chapter 3 reviews some existing calibration procedures and systematic error validation methods. In chapter 4, the methodologies on ALS boresight calibration, systematic error validation and remaining systematic error recovery are described. The test data is also introduced in this chapter.

Chapter 5 presents experimental results. Comparisons on the computed results between manual and automatic measurement of correspondence are shown, followed by the systematic error validation by using a surface matching method and systematic errors recovery. Remaining systematic error recovery is performed by applying the 3-D similarity transformation as well as the strip adjustment with three parameters. Chapter 6 concludes this research with comments and proposes recommendations for future research on this topic.

CHAPTER 2

BACKGROUND

2.1 Airborne LiDAR

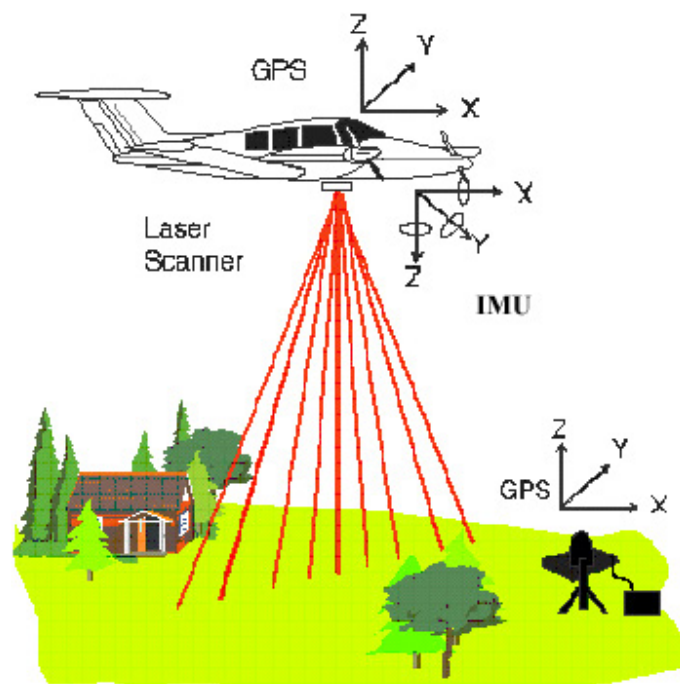
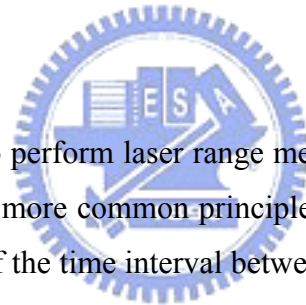


Figure 2. 1: Basic components of an ALS system (ASPRS, 2000)

Airborne LiDAR, also known as airborne laser scanning (ALS), integrates several surveying technologies (Figure 2.1). The basic components include: a Global Positioning System (GPS) receiver and an Inertial Measurement Unit (IMU) as the navigation component, and a laser range finder and a scanner as the remote sensing component (Wehr and Lohr, 1999). To function at maximum accuracy, each component must be properly calibrated and the relationship between the components needs to be determined. Each basic component of an ALS system is sequentially introduced in the following sections.

2.1.1 Ranging

Laser is an acronym for Light Amplification by the Stimulated Emission of Radiation. Laser uses atoms or molecules to store energy and to emit that energy as light. This is accomplished by energizing (pumping) the electrons in the atoms of a laser medium to an excited state by an energy source. The excited atoms are then “stimulated” by external photons to emit the stored energy in the form of photons (stimulated emission). The emitted photons have the frequency characteristics of the atoms and they travel in phase with the stimulating photons. These photons in turn stimulate other excited atoms, which release more photons. Light amplification is achieved as the photons move back and forth in the laser cavity, triggering further stimulated emissions. The photons generated in this fashion are emitted in the form of an intense, directional, and monochromatic laser beam through the partially reflective mirror (Filin, 2001). Therefore, the laser ranging unit contains the laser transmitter and the receiver. The two units are mounted so that the received laser path is the same as the transmitted path. This ensures that the system will detect the target which it illuminates (Morin, 2002).



Two principles are used to perform laser range measurement: (1) pulsed ranging, and (2) continuous wave ranging. The more common principle is pulse ranging. Pulsed laser ranging is based on the measurement of the time interval between the pulse transmission and its return. A short pulse with high peak power is transmitted from the system; the travel time is measured by counting returned photons. The traveling time of a light pulse is: $\rho = \frac{cT}{2}$, with T, the round-trip travel time; ρ , the range; and c, the velocity of light.

In comparison, the continuous wave ranging principle is based on the phase difference between the transmitted and received signal backscattered from the object (Wehr and Lohr, 1999). This principle is applied to lasers that continuously emit light. It is therefore called continuous wave (CW) ranging (Baltsavias, 1999b; Wehr and Lohr, 1999). In order to avoid phase ambiguities, the transmitted signal is modulated to multiple frequencies so that long wavelengths enable one to determine the coarse range. The shorter the wavelengths are, the more precise the range. The relation between phase and range is $\rho = \frac{\lambda}{4\pi} \Phi$, with λ , the laser

wavelength, and ϕ , the measured phase. There is only one CW-laser scanner, employed in commercial airborne laser scanning, which was developed by the Institute of Navigation, University of Stuttgart (Wehr and Lohr, 1999).

In current commercial ALS systems, pulsed lasers are often used. Pulse lasers are usually solid-state lasers that are based on a Neodymium Yttrium Aluminum Garnet (Nd:YAG) laser. The selection of the optical wavelength of the laser is dependent on the overall laser scanning system design. For Nd:YAG lasers, the fundamental wavelength is 1064 nm (near-infrared range), with a double frequency wavelength of 532 nm (green range). The transmitted energy interacts with the target surface and permits the derivation of range and reflectance measurement. The intensity of the reflected near-infrared signal can be used to form an image of the measured area. Objects with high reflectivity such as retro-reflective paint or cement contrast distinctly with objects of low reflectivity such as coal or soil.

The footprint of the laser is a function of the flying height of the platform and the divergence of the laser beam. The narrow divergence of the laser beam defines the instantaneous field of view (IFOV) of the sensor. The IFOV is typically between 0.3 mrad to 2 mrad (Wehr and Lohr, 1999) for a spatially coherent beam of laser light. The theoretically physical limit of the IFOV is determined by diffraction of light, which causes image blurring. Therefore, the IFOV is a function of the transmitting aperture D and the wavelength of the laser light λ . For spatially coherent light, the $\text{IFOV} = 2.44 \lambda / D$. For example, at a flight height of 500 meters, this will result in a laser footprint of 30 cm in diameter on the ground.

2.1.2 Scanning

Due to the very narrow IFOV of the laser, the optical beam has to be moved across the flight direction in order to obtain area coverage required for surveying. Thus, the second component of an airborne LiDAR, i.e. the laser scanning, deflects a ranging beam in a certain pattern so that an object surface is sampled with a high point density (Wehr and Lohr, 1999).

Compared to profiling systems, the advantages of scanning systems are clear: for mapping purposes, both the relatively wide range area covered by each swath and the high

density of laser points are optimal. To perform a scan of a surface, the laser beam has to be moved. This is achieved with rotating mirrors or other means to provide across-track scanning. In addition, the motion of the platform provides along-track scanning. The total across-track scanning angle defines the swath width or field of view (FOV).

The scan pattern on the ground depends not only on the laser scan pattern, but also the flying direction, the flight speed, and the terrain topography. Although the ground point spacing is not deterministic, it basically follows a general shape of the scanning mechanism (Wehr and Lohr, 1999; Morin, 2002).

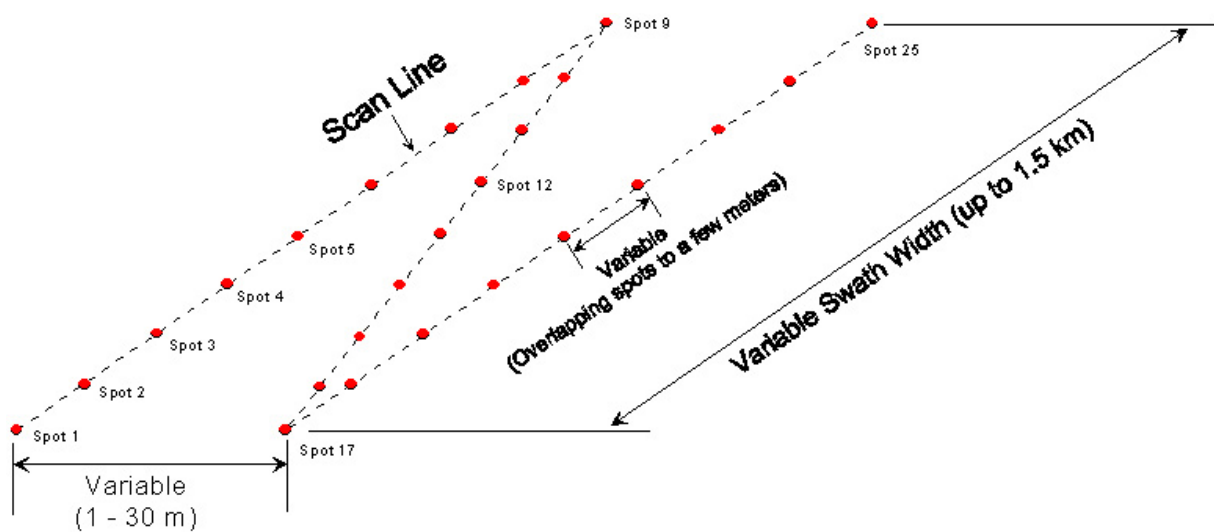


Figure 2.2: Oscillating mirror scanning pattern (Carter et al., 2001)

There are three major scanning techniques employed in different commercial ALS systems. The first and the more popular method is to use an oscillating mirror. Commercial systems such as Leica Geosystems ALS and Optech ALTM, employ this scanning method. With this method, the mirror is rotated back and forth, which generates the effect of creating a zigzag line (bidirectional scan) of scan pattern on the ground (Figure 2.2).

The advantage of this method is that the mirror is always pointing towards the ground. Consequently, data collection is continuous. The user can generally control the mirror's field of view and scan rate. However, there are several disadvantages. The changing velocity and acceleration of the mirror cause torsion between the mirror and the angular encoder. The

changing velocity also implies that the measured points are not equally spaced on the ground. The point density increases at the edge of the scan field where the mirror slows down, and decreases at nadir.

An additional advantage of the oscillating mirror is an ability to compensate for aircraft motion. Across all forms of ALS scanners, the scan pattern on the ground shows the effect of the aircraft motion (particularly roll). The edges of the scan are ‘wavy’ (caused by roll) and the areas of the scan field can appear compressed (caused by pitch). For mission planning, this is problematic since excessive aircraft motion can create gaps in the target measurement area. The points at the swath borders therefore exhibit other characteristics and are sometimes removed from the raw data set (Wehr and Lohr, 1999; Carter et al., 2001).

Oscillating mirrors can be integrated with real-time output of the IMU component to correct for roll type errors. As the aircraft rolls in one direction, the scanner control hardware module compensates the motion resulting in a more stable scan pattern (Morin, 2002).

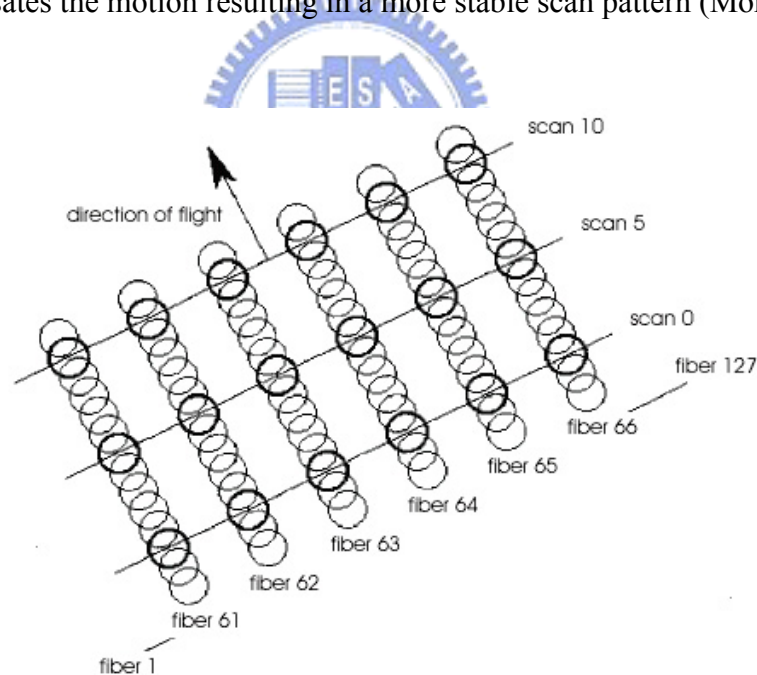


Figure 2.3: Nutating scanner pattern (Lohmann, 1999)

Next, the second scanning method is used by TopEye based on a fiber-optical array (Lohmann, 1999; Wehr and Lohr, 1999; TopEye AB, 2006). Rather than moving a mirror to direct the laser onto the ground, a small nutating/rotating mirror is used to direct a laser into a

linear fiber-optical array. The array transmits the pulse at a fixed angle onto the ground (Figure 2.3). The significant characteristic of the fiber scanner is that the transmitting and the receiving lenses are identical (Wehr and Lohr, 1999). An identical fiber line array is mounted in the focal plane of the transmitting and the receiving lenses.

The advantage of this system is that with fewer and smaller moving mechanical parts, higher scanning rates can be achieved. This is not possible with conventional mirror scanners. These systems typically have a sufficient scan rate such that points overlap in the along-track position. A disadvantage is that the FOV is currently much smaller than a rotating mirror (for example, +/- 7 degrees for the TopoSys fiber scanner) and the across-track positions are fixed (Wehr and Lohr, 1999). Thus, the only variable is the aircraft flying height.

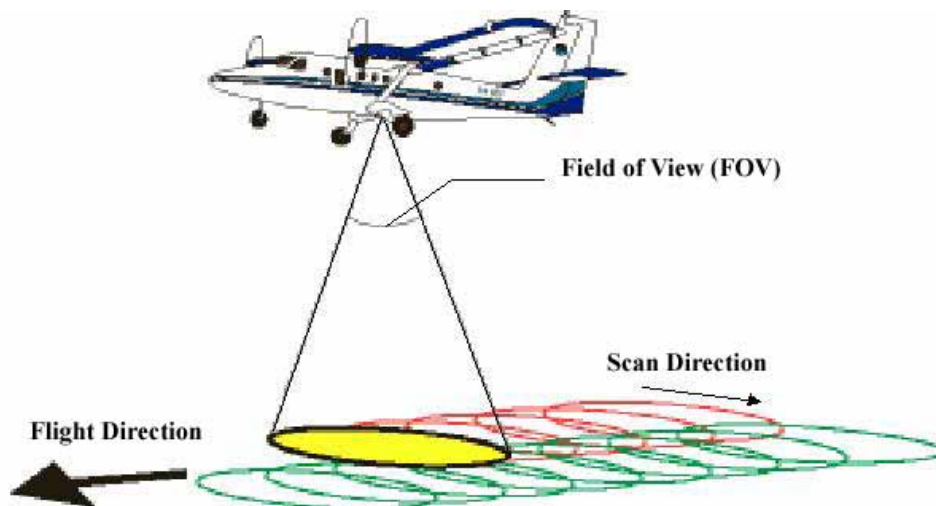


Figure 2.4: Elliptical scanner pattern (Carter et al., 2001)

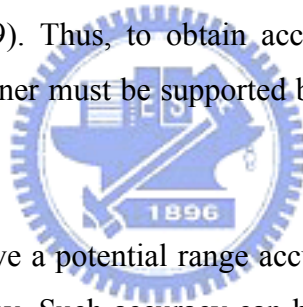
The third scanning method is the Palmer or elliptical scanner (Wehr and Lohr, 1999). The system employs two mirrors to move the laser along an elliptical path around the aircraft (Figure 2.4). When the scanning is projected on the ground, an approximately elliptical scanning pattern can be observed. The advantage of this system is that most of the measurement points on the ground are scanned twice with the conical scanning pattern, once in the forward view and a second time in the backward view. The scanning allows the areas that were occluded on the first pass to be measured on the second. Furthermore, the redundant

information on the same ground spot can be favorably used to calibrate the scanner and the position/orientation (POS) as far as the pitch angle is concerned (Wehr and Lohr, 1999).

Disadvantages include the increased complexities of two mirrors, in addition to the uncertainties that two angular encoders would converge on a derived point location. Compared to the line scanning, the spiral shape distribution of the laser points produces an irregular point distribution. Furthermore, the point density is changing. It is denser at the ends of the swath laser points than at the center of the swath.

2.1.3 Position and orientation system

The last subsystem measures the position and the attitude of the ALS system. The laser scanner measures only the line-of-sight vector from the laser scanner aperture to a point on the earth surface. The 3-D position of this point can only be computed under the condition that the position and the orientation of the laser system are known with respect to a coordinate system (Wehr and Lohr, 1999). Thus, to obtain accurate range measurements in a given coordinate system, a laser scanner must be supported by the Position and Orientation System (POS).



Because laser scanners have a potential range accuracy of better than 1 dm, POS should allow at least the same accuracy. Such accuracy can be achieved only by an integrated POS consisting of a differential GPS and an IMU system. The absolute positioning of the ALS platform comes from GPS. Differential GPS is generally used with ground reference stations. Most systems employ an IMU to determine the attitude (Baltsavias, 1999b; Krabill et al 2000). Geocoding of laser scanner measurements requires an exact synchronization of all system: laser scanning data, IMU and DGPS.

The features of the IMU (attitude determination, high data rate, e.g. often 200Hz) neatly complement the features of a DGPS system (fairly low data rate 2-10 Hz, high positional accuracy). Together, they provide highly accurate and stable navigation information. Among commercial systems, the Applanix navigation system is often used for the navigation unit (Leica, 2002; Optech, 2002; Morin, 2002). The individual sensor measurements then go into the observation model to form the target coordinates.

2.1.4 Determination of laser point

After an ALS surveying flight, two data sets are available: the POS data and the laser ranges with the instantaneous scanning angles. To achieve high accuracy in the position of laser points, some systematic parameters must be considered. These parameters are the three mounting angles of the laser scanner frame. They are the roll angle with respect to the platform-fixed coordinate system, the pitch angle (the position of the laser scanner) with respect to the IMU, and the heading angle (the position of the IMU) with respect to the GPS. This so-called calibration data can be derived from laser scanner data, whereby certain reference areas are flown-over in different directions (Wehr and Lohr, 1999). The details on ALS calibration will be discussed in Section 2.3 and Section 4.1.

The laser points in the coordinate system of mapping frame can therefore be computed with the help of the three data sets: calibration data and mounting parameters, laser distance measurements with their respective scanning angles and POS data. The individual error contributes to the accuracy of the target coordinate (revealed in equation 4-1). A review of the literature concerning calibration and quality assessment shows that there is no standard procedure for error modeling. The type of modeled errors varies from one researcher to another, and usually only few error sources are modeled (see Section 3.1). Schenk (2001) analyzes the potential error source and presents a model to their effects.

2.2 Potential error sources

Three components of the laser system, namely, GPS, IMU and ranging, are sources of systematic errors. Errors may be intrinsic properties of each component; additional errors are the consequence of their integration (Filin, 2001). The errors of an ALS system originate from its three components: the laser scanning, navigation, and control units.

2.2.1 Laser scanning system

For a pulse modulation laser, the design of the scan mirror results in the scanning error. The working behavior and the magnitude of the scanning error vary across different commercial ALS systems. For example, the error caused by the changes in velocity typically associated with oscillating mirrors is one of the most serious scanning errors in a Leica ALS

system. The torsion effect of the scanning error on the derived ground point results in a bowing along the across-track profile of an ALS strip.

During normal operation, the scan mirror is in a continuous motion. Due to the nature of the oscillating scan pattern, however, the mirror is repeatedly accelerated and decelerated in order to reverse its direction. Since the mirror and encoder have mass, they will have momentum during its motions (Morin, 2002). The magnitude of momentum varies depending on the angular position of the mirror.

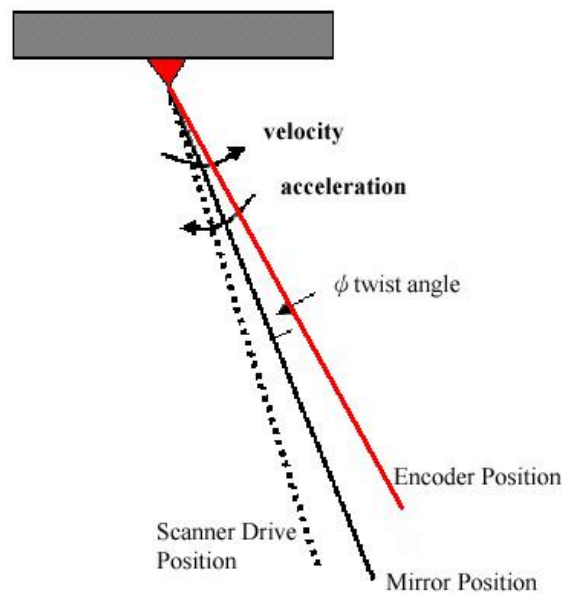


Figure 2.5: Component Lag (Morin, 2002)

The difference in angular position between the scan mirror and the encoder causes a mis-registration of the observed distance. As seen in Figure 2.5, the mirror sends the laser pulse in the direction of the solid black line, but the encoder perceives the pulse to be from the direction of the solid red line, which lags behind the black line by a twist angle of ϕ . Over a flat terrain, the range measurement at the mirror position will be shorter than the range measured at the encoder position. As a result, an incorrect short range is recorded at the encoder position.

The difference between the true distance at the encoder direction and the measured distance from the mirror increases proportionally with the scan angle, the FOV and the scan rate. The observed effect in the data is the strip bowing, which is also commonly referred to as the “sensor smile” (Figure 2.6).

The elevation differences from the torsion effect reach a maximum at the edge of the field of view. The “smile” can be a frown, however, depending on the particular design of the scanner. If the encoder is placed before the mirror, then the mirror will lag behind, and the registered distances will be too long. Such error produces a downward bow, or a frown. The torsion causes a small but systematic misreading of the angle, which is manifested by the ends of the scan rising too high or dropping too low. Due to the systematic nature of this error, it can be modeled and removed during the calibration process (Morin and EL-Sheimy, 2002).

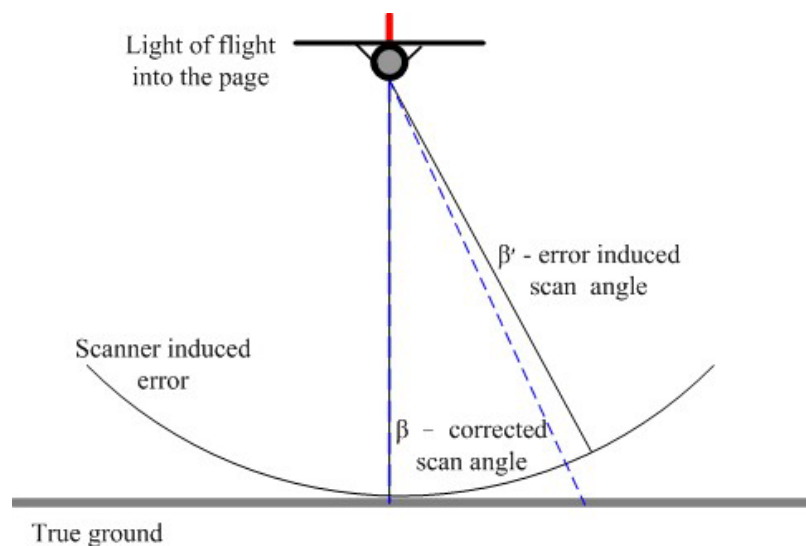


Figure 2.6: Torsion error

2.2.2 Navigation system

In regards to position errors, Burman (2002) found tropospheric delay to be a potential source of error. The tropospheric delay is a function of the distance between the ALS system and the GPS base station. Solutions that incorporate multiple base stations over a mission may reduce this effect (Filin, 2001). In addition to tropospheric delay, most errors in the GPS system are dependent on the operating conditions and set-up (Morin, 2002). These include the reference station baseline, the number of satellites in view, and whether precautions to avoid

loss of lock were taken during flight time. Ambiguity resolution is done before the mission begins, while the platform is on the ground. If loss of lock were to occur during the flight, the result would be catastrophic for the ALS system, and would require an in-flight re-initialization. With correct ambiguity resolution, post-processing position accuracy is typically 5-15 cm (Wehr and Lohr, 1999).

The IMU system contributes several types of errors in the ALS system. The overall accuracy of the navigation attitude will depend on the quality of the IMU. Commercial systems often employ civilian versions of sensor such as those from Applanix Corporation (Applanix, 2004). Current models (POS 510) from Applanix have the absolute accuracies of 0.005 degrees in pitch and roll, and 0.008 degrees in heading. However, the terrain can affect the accuracy of IMU. Areas with a large amount of geoidal undulation will require additional processing to obtain accurate attitude information (Krabill et al., 2000).

In addition to the absolute accuracy, IMU gyroscopes are subject to sensor drift. For the Applanix sensors, gyro drift rates can vary between 0.1 – 0.75 degree/hour (Applanix, 2004). The gyroscope measurements contain biases, drift error and noise. The navigation processing software will attempt to remove the biases and drifts based on previous calibrations but the noise components remain. Over a long measurement time, strips may exhibit an apparent bend or torsion. Due to the systematic nature of this type of error, it can be modeled by a time-dependant parameter determined in a post-flight adjustment. However, the effect of this gyro error does not have a stable or deterministic property. To compensate for this error, an adjustment must be made for each strip (Morin, 2002).

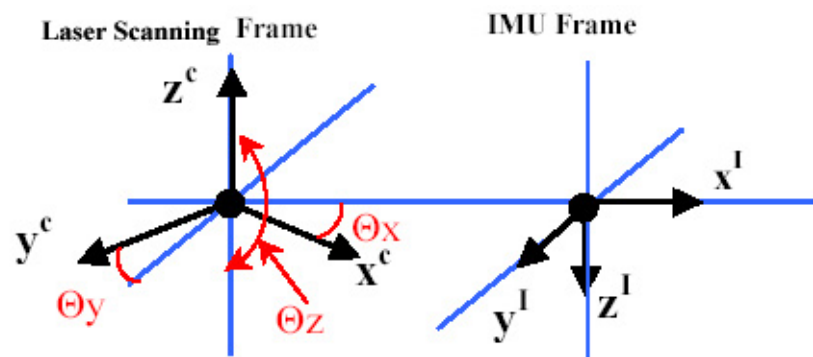


Figure 2.7: Laser scanning system/IMU boresight (Mostafa, 2001)

When using multi-sensor systems, such as an airborne laser scanning system, a number of new calibration requirements arise, namely laser scanning system and boresight calibration. Boresight is the physical mounting angle between an IMU and a laser scanning system that theoretically describe the misalignment angles between the IMU and the laser scanning system frames of references as shown in Figure 2.7 (Mostafa, 2001).

The boresight angle is the largest source of systematic error in an ALS system. It has been observed empirically that these misalignment errors are often relatively small (0.1-3 degrees). An incorrect boresight calibration will affect the position of the derived laser points. Errors induced by the misalignment are a function of flying height, scan angle and flying direction – and must be addressed before an ALS system can be practically deployed.

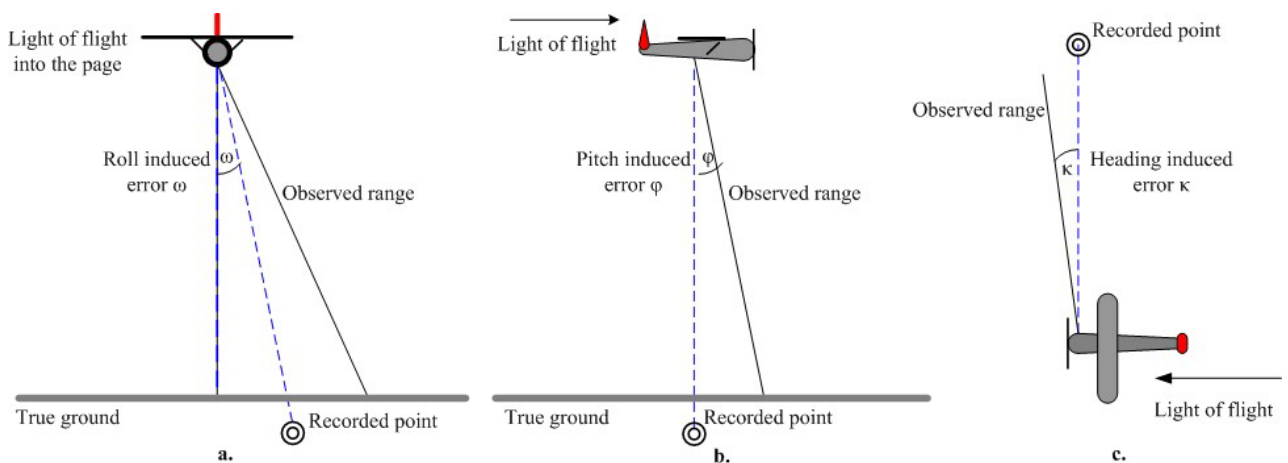


Figure 2.8: Boresight induced errors

For example, at a platform altitude of 700 meters and an off-nadir scanning angle of 15 degrees, a misalignment of 0.1 degrees (roll) will result in a height error of 32 cm and a planimetric error of 131 cm (Krabill et al., 2000). These errors are readily apparent in overlapping ALS data. Comparing areas with elevation gradients (buildings, hills etc) will reveal inconsistencies. Each component, i.e. roll, pitch, and heading, of the boresight errors is illustrated in Figure 2.8a, 2.8b and 2.8c, respectively.

The misalignment between the laser and the IMU causes each laser observation to be registered with an incorrect aircraft attitude. A *roll* error also causes a slant range to be incorrectly registered. The elevation differences tend to increase with a larger scan angle (Figure 2.8a). The *pitch* error (Figure 2.8b) results in a laser slant range to be recorded as nadir. As the slant range becomes longer, the entire strip tends to be pushed down. The *heading* error induces a skewing in each scan line (Figure 2.8c).

Unlike a photographic image, a boresight error affects each observation and cannot be removed by applying a simple affine transformation to the entire strip (Leica, 2003a). Instead, the differences must be modeled by observing the induced errors from the position of control points or common feature points. Given that these errors are correlated with flying direction, they can be decorrelated by observing targets recorded from different directions. The mathematical model and flight planning for boresight calibration are described in Section 4.1.

2.2.3 Time error

A persistent timing problem in an ALS system would be the clock measurement error in a pulsed system that detects the pulse transmission time. For a path distance of 1500 meters (750 m transmit and return), the time delay would be 5×10^{-6} s. A 1% error in the clock (5×10^{-8} s) would result in a range error of 7.5 meters. Fortunately, all commercial systems have a typical accuracy between 0.05 ns and 0.2 ns that is better than the time delay error (Baltsavias, 1999b). This corresponds to a laser ranging accuracy of 1.5 cm. Depending on the pulse rate, clock drifts and biases may come into account. At present, they can be modeled during the calibration set-up (Krabill et al., 2000). After the systematic errors are removed, the common accuracy of an ALS laser range finder taking measurements from 500 meters above ground level is 1.5 – 2cm (Leica, 2002; Optech, 2002; Morin, 2002).

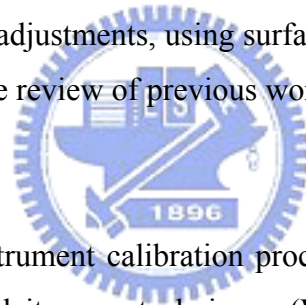
2.2.4 Integration errors

For accurate target determination, all measurements must be referenced to a common time epoch. Each major sub-component has its own timing system, which can be coordinated with GPS time. For accurate integration, clock offsets and drifts must be determined through calibration. Any time delays must be known or they will introduce errors in the integration.

Further, the sub-systems take measurements at different rates. The GPS system typically operates at 2 Hz, IMU at 200 Hz and the laser measures at 10-70 kHz (Optech, 2004; Leica, 2004a). Navigation information is interpolated by applying Kalman filter to match the laser measurements. In normal ALS flight conditions, the IMU data usually smooth the GPS data, leading to more stable results. In more turbulent conditions, interpolation errors may lead to target determination errors. In such conditions, a lower accuracy of the ALS system results (Morin, 2002).

2.3 Calibration problem

The calibration of an ALS system is a complicated task. It is complicated because the ultimate goal is to identify all the systematic errors to the extent that only random errors remain in correcting the raw laser point clouds (Schenk, 2001). Despite the need to determine calibration parameters specific to each ALS system, there is currently no standard method of undertaking the task. Each laser scanning firm has its own procedure for calibration. Techniques vary from manual adjustments, using surface constraints, to forming least squares adjustments (Morin, 2002). The review of previous works on this issue is described in Section 3.1.1.



There are no standard instrument calibration procedures. Each equipment manufacturer and ALS group has developed its own techniques (Wehr and Lohr, 1999). The boresight calibration for the Optech ALTM includes the estimation of the scanner roll and pitch bias corrections, a scanner scale correction, a scanner offset correction, and a timing (ranging) correction (Gutierrez, et. al, 2001). These corrections were initially measured in the manufacturer's laboratory facility and refined by flight testing.

For the Optech ALTM system, the current boresight calibration procedure requires an enormous building and a calibration site. The building, which is used to calibrate the misalignment parameters, has to be at least 80 meters in length and 5 meters in height. In addition, a flat runway that is 1,000 meters long and 50 meters wide is usually designed to calibrate the scale, elevation offset and timing correction. The control points on the roof and on the ground need to be surveyed. Essentially, the method involves flying the ALS sensor over a series of control points or a known surface. The profile from the ALS data strip is

compared with that from a known surface. As shown in Figure 1.1, the effects of the misalignment are readily visible by an offset between the two profiles. A user then manually applies corrections and reprocesses the data. The comparison between the two profiles demonstrates the effects of the corrections.

For the Leica ALS system, roll and pitch are determined by comparing profiles over flat areas. The parameters are changed until the overlapping areas coincide. Heading can be determined by examining areas with large elevation gradients such as buildings. Two flight lines are flown over a building area: one flight line captures the building on the far right of the FOV, whereas the other flight line captures the building on the far left. The errors in the heading induce a distortion in building location. By changing the heading parameter, the distortions will change. The heading is altered until the sides of the building align. Showing a more comprehensive understanding on the boresight misalignment calibration, the design and measurement to each angle is presented as follows for the Leica ALS (Liu et al., 2005).

The calibration process involves several steps. The first step is to calibrate individual system components in the laboratory, followed by a system calibration on the platform (i.e. mounting parameters). The next step is boresight (in situ) calibration before and after the mission. If necessary, additional boresight calibration is required even between missions. In practice, however, such an undertaking is impractical due to time and expense considerations, and unnecessary due to the relative stability of the calibration parameters and the magnitude of certain error sources. Most of the calibration parameters are determined by the supplier when the instrument was in the factory/laboratory and should remain stable for the operational lifetime of the unit.

There are three categories of calibration procedures: pre-flight methods, post-flight calibration and post-flight adjustment. The pre-flight methods cover laser range bias determination, GPS initialization, IMU initialization, and so forth. Among the pre-flight methods, the initialization of navigation equipment such as GPS and IMU is a standard set-up function of an ALS system. In contrast, scanner biases and error sources that are relatively stable such as range finder biases are not commonly applied.

Some calibration parameters, notably the boresight angles, cannot be measured directly and must be derived from the ALS data. The parameters may also change if the unit undergoes a strong physical shock or extreme temperature change (Leica, 2003). The angle misalignment between the IMU body frame and the scanner frame is the largest source of error. However, the angle misalignment is a relatively stable type of error, so they can be determined in the field.

The sequence on the calibration of boresight misalignment is roll, torsion, pitch and heading while the calibration is being manually adjusted. Firstly, based on the formation of roll error (Figure 2.8a), two flight lines flown in the opposite direction are chosen to measure the roll (Figure 2.9a). A flat site on the edge of FOV, e.g. site P , will have the most significant height discrepancies from the across-track direction (Figure 2.9b). The height difference, h , can then be measured. If the distance between P and nadir line, i.e. r , is known, the roll can be computed.

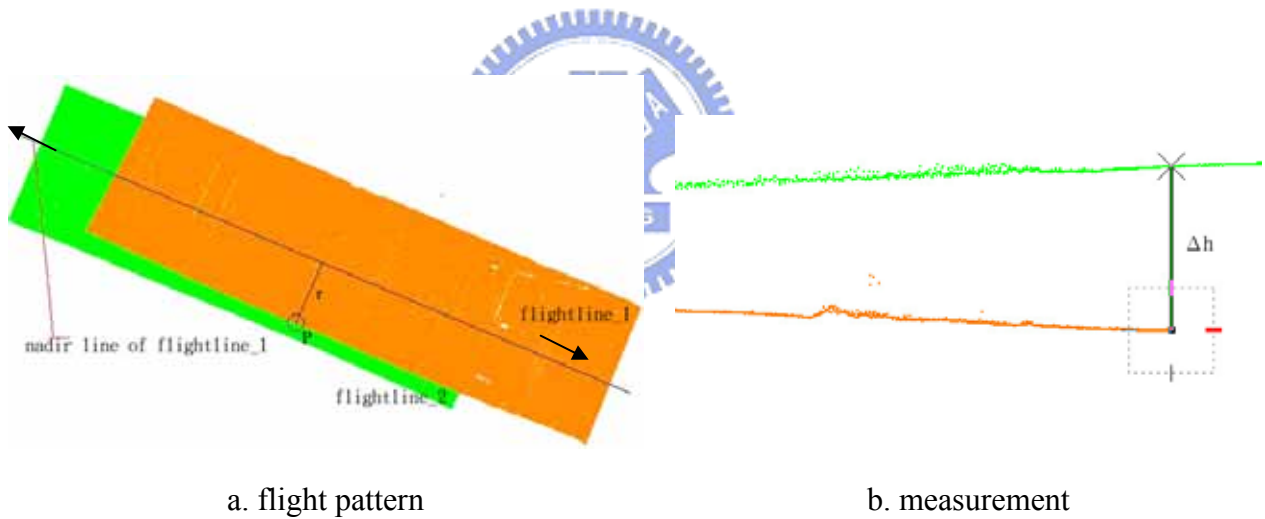


Figure 2.9: Boresight misalignment - roll

$$Roll_{\Omega} = \tan^{-1} \frac{\Delta h / 2}{r} \quad (2-1)$$

For example, with $h=18.639$ m, flight altitude $H=600$ m, FOV=45 degrees, $r=214.50$ m, $Roll$ is equal to 0.04352 radian. The updated roll angle then replaces the old (or uncalibrated) one. The coordinate of point clouds with other angles fixed are subsequently re-calculated. These procedures need to be repeated until h is small enough.

The induced error by torsion is easily found at the edge of the field (Figure 2.6). Therefore, only the edges of the swath are used to compute the torsion error. For example, point clouds are extracted with the minimum angle of -25 degrees and the maximum angle of -15 degrees. The average elevation discrepancies can then be computed to compare with ground control points. Adjust the torsion value and reprocess the point clouds until the average height difference approaches zero.

Table 2.1: Measured elevation offset versus torsion value

Torsion (Newton-m)	-60,000	-40,000	-30,000	-20,000	-10,000	-5,000	-1,000	0
Elevation Offsets (m)	0.069	0.069	0.084	0.119	0.214	0.450	2.094	0.034
Torsion (Newton-m)	1,000	5,000	10,000	20,000	30,000	40,000	50,000	60,000
Elevation Offsets (m)	-2.061	-0.374	-0.169	-0.066	-0.032	-0.015	-0.005	0.002

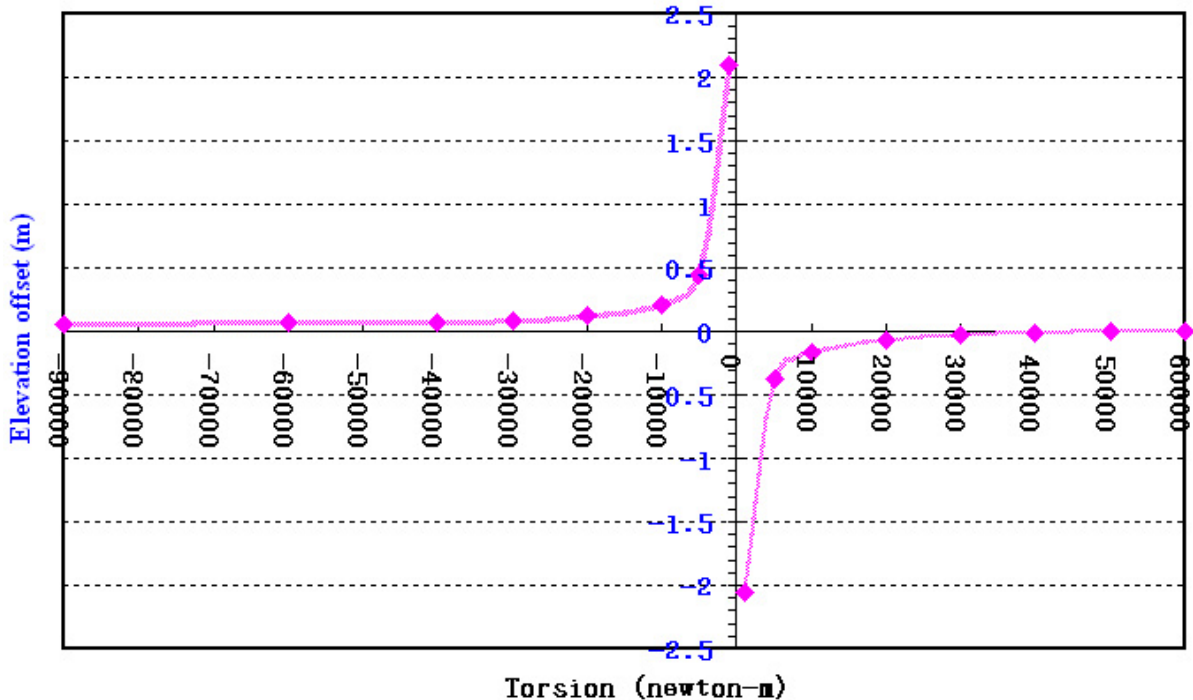


Figure 2.10: Torsion value versus elevation offset

Note that torsion is not linear and its value should be changed in multiples of 5,000 to start off (Hentschel, 2005). The elevation offset versus torsion value is depicted as Table 2.1 and Figure 2.10. Then check point clouds by processing the other edge of the swath with the minimum angle of 15 degrees and the maximum angle of 25 degrees. This can ensure that the edges of the data are in the correct position.

As shown in Table 2.1 and Figure 2.10, the elevation discrepancy is 2 mm when the torsion value is 60,000. This manually interpreted torsion constant will hereafter be used as one of the boresight misalignment parameters.

Next, according to the characteristic of pitch error (Figure 2.8b), an elevation discrepancy can be revealed from two strips with different altitude (for example, 600 m and 1000 m). As shown in Figure 2.11a, the site with a gable roof located on the nadir line will be selected to compute the pitch error. The pitch can be computed when the elevation difference, Δh , is measured (Figure 2.11b).

$$Pitch_{\phi} = \cos^{-1} \frac{\Delta H}{\Delta H + \Delta h} \quad (2-2)$$

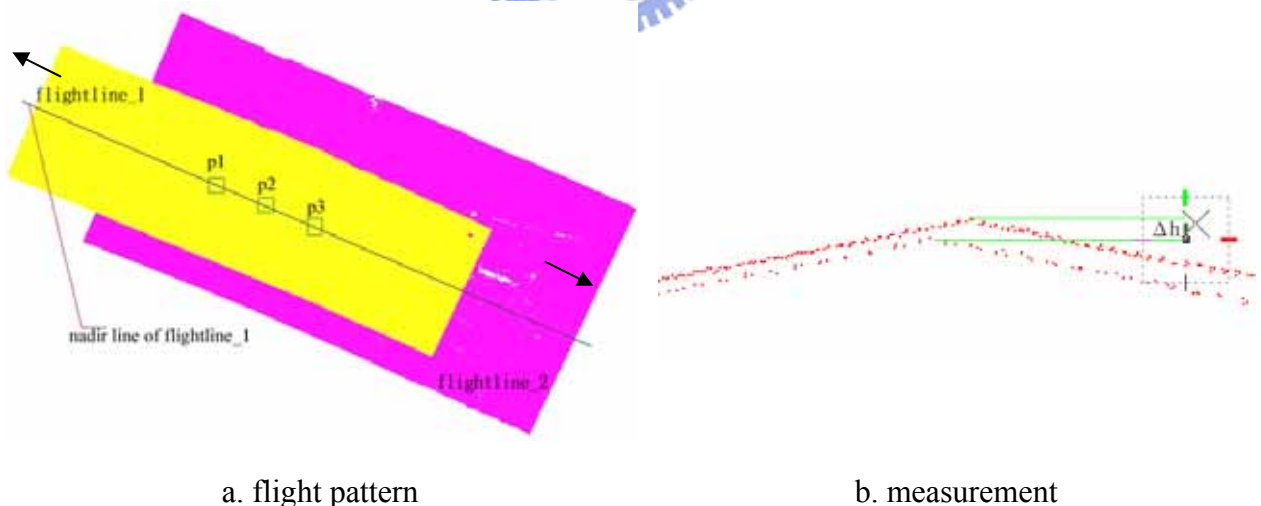


Figure 2.11: Boresight misalignment - pitch

For instance, with $h=2.95$ cm, difference of flight attitude $H=400$ m, then $Pitch$ is equal to 0.0118 radian. The updated pitch angle then replaces the old (or uncalibrated) one. The coordinate of point clouds with other angles fixed are subsequently re-calculated. Correspondingly, these procedures need to be repeated until h is small enough.

To maximize the differences induced by the heading error, flight lines should be flown perpendicularly to each other based on the behavior of the heading error (Figure 2.8c). Those sites distributed on the corners (e.g. $P1$, $P2$, $P3$, or $P4$ in Figure 2.12a) of the overlapping area can be selected to measure the planimetric shifts. The planimetric difference, i.e. Δx , is then measured while drawing a profile parallel to flight direction (Figure 2.12b). The heading parameter can be derived if the slant distance between the center of scanner and the selected ground feature, i.e. l , was calculated.

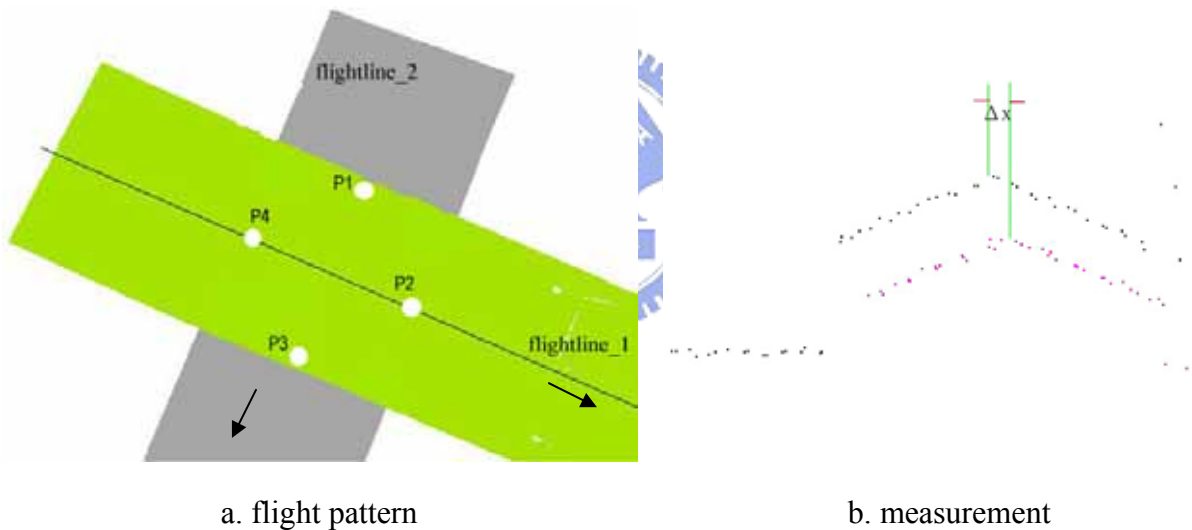


Figure 2.12: Bore sight misalignment - heading

$$Heading_k = \tan^{-1} \frac{\Delta x}{l} \quad (2-3)$$

With $x=0.68$ m, $H=600$ m, $FOV=45$ degrees, $l=649.44$ m, then $Heading$ is equal to 0.00105 radian. As before, the updated heading angle is used to replace the old (or uncalibrated) one. The coordinate of point clouds with other angles fixed are subsequently re-calculated. Correspondingly, these procedures need to be repeated until the overlapping areas coincide.

Once the misalignment angles are approximated, the scanner errors can be estimated. Their effect manifests as a systematic distortion of the data profile along the control surface. Often a bowing will appear in the profile; where the edges will rise above the known surface. Again, the user applies corrections to reprocess the data depending on the error model used in the sensor. The correction continues until the edges flatten out. The manual calibration procedure can take several iterations and require a considerable amount of time (Morin, 2002). The end results are usually only judged 'by eye' as the method does not produce any direct statistical information about the solution. Further, the solution may be biased by any local errors or variations in the observed surface, since the calibration was performed with a small portion of the data. Thus, the calibration may not be the best solution for the entire dataset.

In general, the ALS calibration is a time-consuming task. To achieve higher accuracy, Morin (2002) proposed a new calibration method to allow the determination of the boresight misalignment angles. The mathematical model and the flight planning will be described in Section 4.1. This research will evaluate this method and suggest a proposal for improvement.

2.4 Systematic error validation

Once the updated calibration parameters are derived, the 3-D coordinate of point clouds based on a mapping frame can be re-computed. To validate the point clouds, it is necessary to evaluate the accuracy of the calibration parameters and estimate the magnitude of the remaining systematic errors. Presently, most of the commercial systems use ground reference points to validate the high discrepancies of calibrated ALS data. Such system error validation method suggests the following: (i) the validation of height offset is easily implemented, (ii) DEM is generally the most serious for ALS survey, and (iii) planimetric shift is not applicable to derive directly by using ground control points.

Unlike photogrammetry, the ALS data are not collected on a frame or strip basis, but rather point-by-point. The aircraft is at a new position and orientation for each point of data collection. The points are distributed in a random manner along the scanning track. For example, the scanning track may have a zigzag shape for oscillating scanning. The user has no control over what the laser hits; thus signalized control points are sometimes difficult to detect.

The laser beam diverges when it passes through the atmosphere. With the accuracy of planimetry being much worse than height accuracy, the accuracy assessment on planimetry is also emphasized on the demand of applications. Therefore, several methods have been developed to help determine tie points between ALS strips. The simplest way of collecting tie points is to measure them manually with grid data. The user picks off common features between the overlapping strips or attempts to measure known control points (Kilian et al., 1996; Lee et al., 2003). Such method requires an experienced operator and is time consuming. The reviews on this topic are briefly discussed in Section 3.1.

In comparison, this research addresses a critical issue in systematic error validation that has yet to be examined – how to establish the correspondence between the two overlapping strips, or the correspondence between the laser points and the spots on the ground they illuminate. With the correspondence being established, the calibration becomes an ordinary adjustment problem (Filin, 2001). A surface-based matching to establish the correspondence and validate the planimetric shifts as well as the elevation discrepancies is presented in this research.

